

Videofluoroscopic Validation of a Translational Murine Model of Presbyphagia

Teresa E. Lever · Ryan T. Brooks · Lori A. Thombs ·
Loren L. Littrell · Rebecca A. Harris · Mitchell J. Allen ·
Matan D. Kadosh · Kate L. Robbins

Received: 13 January 2015 / Accepted: 25 February 2015
© Springer Science+Business Media New York 2015

Abstract Presbyphagia affects approximately 40 % of otherwise healthy people over 60 years of age. Hence, it is a condition of primary aging rather than a consequence of primary disease. This distinction warrants systematic investigations to understand the causal mechanisms of aging versus disease specifically on the structure and function of the swallowing mechanism. Toward this goal, we have been studying healthy aging C57BL/6 mice (also called B6), the most popular laboratory rodent for biomedical research. The goal of this study was to validate this strain as a model of presbyphagia for translational research purposes. We tested two age groups of B6 mice: young (4–7 months; $n = 16$) and old (18–21 months; $n = 11$). Mice underwent a freely behaving videofluoroscopic swallow study (VFSS) protocol developed in our lab. VFSS videos (recorded at 30 frames per second) were analyzed frame-by-frame to quantify 15 swallow metrics. Six of the 15 swallow metrics were significantly different between young and old mice. Compared to young mice, old mice

had significantly longer pharyngeal and esophageal transit times ($p = 0.038$ and $p = 0.022$, respectively), swallowed larger boluses ($p = 0.032$), and had a significantly higher percentage of ineffective primary esophageal swallows ($p = 0.0405$). In addition, lick rate was significantly slower for old mice, measured using tongue cycle rate ($p = 0.0034$) and jaw cycle rate ($p = 0.0020$). This study provides novel evidence that otherwise healthy aging B6 mice indeed develop age-related changes in swallow function resembling presbyphagia in humans. Specifically, aging B6 mice have a generally slow swallow that spans all stages of swallowing: oral, pharyngeal, and esophageal. The next step is to build upon this foundational work by exploring the responsible mechanisms of presbyphagia in B6 mice.

Keywords Deglutition · Deglutition disorders · C57BL/6 · C57 · B6 · Mouse · Murine · Aging · Swallow · Dysphagia · Presbyphagia · Videofluoroscopic swallow study · VFSS

T. E. Lever (✉) · M. J. Allen · K. L. Robbins
Department of Otolaryngology – Head and Neck Surgery,
University of Missouri School of Medicine, One Hospital Drive
MA314, Columbia, MO 65212, USA
e-mail: levert@health.missouri.edu

R. T. Brooks · L. L. Littrell · R. A. Harris
Department of Communication Science and Disorders,
University of Missouri, 308 Lewis Hall, Columbia, MO 65211,
USA

L. A. Thombs
Department of Statistics, University of Missouri,
146 Middlebush Hall, Columbia, MO 65211, USA

M. D. Kadosh
Department of Biological Sciences, University of Missouri,
105 Tucker Hall, Columbia, MO 65211, USA

Introduction

Presbyphagia is an increasingly recognized term describing age-related deterioration of swallow function in *healthy* adults, beginning around the 5th and 6th decades of life [1–5]. Hence, presbyphagia is considered a condition of *primary biological aging* (i.e., senescence) that is distinctly different from dysphagia, which is attributed to *primary disease* such as stroke, neurodegenerative conditions, and head and neck cancer. Common symptoms of presbyphagia include generally slow, delayed, and uncoordinated swallowing that compromises airway protection [3, 6–10]. More specifically, compared to younger adults, healthy older individuals (1) have significantly longer oral [4, 11],

pharyngeal [1, 4, 6, 10, 11], and esophageal [12–14] transit times, (2) require significantly larger bolus volumes to trigger the pharyngeal swallow response [15], and (3) have significantly increased occurrences of delayed pharyngeal swallowing [6, 11, 16, 17], laryngeal penetration [1, 11, 18–20], aspiration [18, 19], and post-swallow residue in the oral cavity [11], pharynx [4, 11, 16, 18], and esophagus [10, 12, 14, 21]. In addition, the anatomical location of the pharyngeal swallow trigger point in older adults migrates inferiorly, with the bolus frequently accumulating deeper in the pharyngeal recesses (valleculae and pyriform sinuses) prior to triggering the pharyngeal swallow response [6, 17]. Data for gender differences in the swallow function of healthy older individuals are scant, but a higher incidence of aspiration among healthy older men has been reported [18].

Although subtle, these age-related changes in swallow function (i.e., presbyphagia) place older individuals at risk for developing life-threatening malnutrition and aspiration pneumonia, particularly when faced with major health conditions, either acute (e.g., stroke, surgery, etc.) or chronic (e.g., neurodegenerative diseases, head and neck cancer, inflammatory diseases, and general frailty), that further compromise the aging swallowing mechanism [2, 3, 22, 23]. However, it is unclear whether presbyphagia is truly a symptom of healthy aging or an early indicator of an age-related disease that has not yet been diagnosed but is associated with dysphagia. This distinction between presbyphagia and dysphagia is of critical importance, given the astronomically growing aging population worldwide.

In America alone, the number of individuals 50 years and older in 2010 was estimated at 99 million, and this number is expected to increase by 15–20 million per decade through 2050 [24]. Moreover, up to 22 % of Americans over 50 years of age [25] and nearly 40 % of Americans over 60 [2, 26, 27] experience dysphagia. These striking statistics substantiate the urgent necessity for extensive research toward understanding the role of primary aging versus primary disease specifically on the structure and function of the swallowing mechanism. However, mechanistic studies of muscles, mucosa, nerves, and brain tissue of the swallowing mechanism throughout the lifespan are not feasible to conduct in humans, due to the invasive nature and high cost of the research methods, as well as the high risk-to-benefit ratio for individuals. As a result, the underlying mechanisms of presbyphagia and dysphagia are largely unknown; therefore, mechanistic targets for treatment interventions remain elusive. To address this major health care problem in the escalating aging population, we have been studying healthy aging C57BL/6 (also called B6) mice, the most popular laboratory rodent for biomedical research [28, 29].

The B6 mouse was created nearly a century ago in the United States and has since become the most commonly

used background strain for studying genetic mutations [30–32]. As a result of its long history in research, the B6 mouse was unanimously chosen in 2001 as the first animal to have its DNA sequenced for comparison with the Human Genome Project [29]. The major appeal of this strain is its longevity—B6 mice often survive more than 24 months without developing tumors or diseases [33]. Thus, this strain is well-suited for studying the biology of primary aging and has been identified by the NIH National Institute on Aging specifically for this purpose [34]. The goal of this study was to validate B6 mice as a robust model of presbyphagia that is well-suited for translational research in health and disease conditions.

An ideal translational mouse model of presbyphagia must demonstrate deterioration in all three stages of swallowing in a manner similar to humans with this condition. Our preliminary work with healthy aging B6 mice identified a significant age-related decline in lick rate after 17 months of age [35] (Fig. 1), assessed using a non-radiographic lick rate assay developed in our lab [36, 37]. In mice, licking is the primary means of ingesting liquid [38], which corresponds to the oral stage of swallowing [36] or Stage I transport (i.e., ingestion into the oral cavity) [37]. Thus, the slower lick rate of otherwise healthy older (i.e., primary aging) B6 mice suggests this strain develops presbyphagia affecting the oral stage of swallowing. We hypothesized that aging B6 mice also develop changes in the pharyngeal and esophageal stages of swallowing resembling presbyphagia in humans. To test this hypothesis, we assessed the oral, pharyngeal, and esophageal stages of swallowing in young (4–7 months) and old (18–21 months) B6 mice using videofluoroscopic swallow study (VFSS) methods.

VFSS is considered the gold standard diagnostic test for concurrent assessment of all three stages of swallowing in humans [39–41]. We recently adapted human VFSS methods for use with mice and other small rodents, referred to as a murine VFSS protocol [42]. The protocol consists of three key components: (1) custom-designed test chambers that permit freely behaving feeding and swallowing in a confined space, (2) specially formulated species-specific recipes that mask the aversive taste/odor of commercially available oral contrast agents, and (3) a step-by-step test protocol that permits reliable quantification of several swallow metrics for each stage of swallowing. In addition, we recently acquired a custom-designed low energy fluoroscopy system called The LabScope (Glenbrook Technologies, Randolph, NJ), which is a miniature X-ray microscope that can magnify and digitally record extremely small regions of interest, such as the swallowing mechanism of a mouse. The LabScope generates a continuous cone-beam of X-rays with low photon energies (15–40 kV) and has a peak tube current of 0.2 mA, producing a maximum power output of 8 Watts. The thin bone and soft tissue of

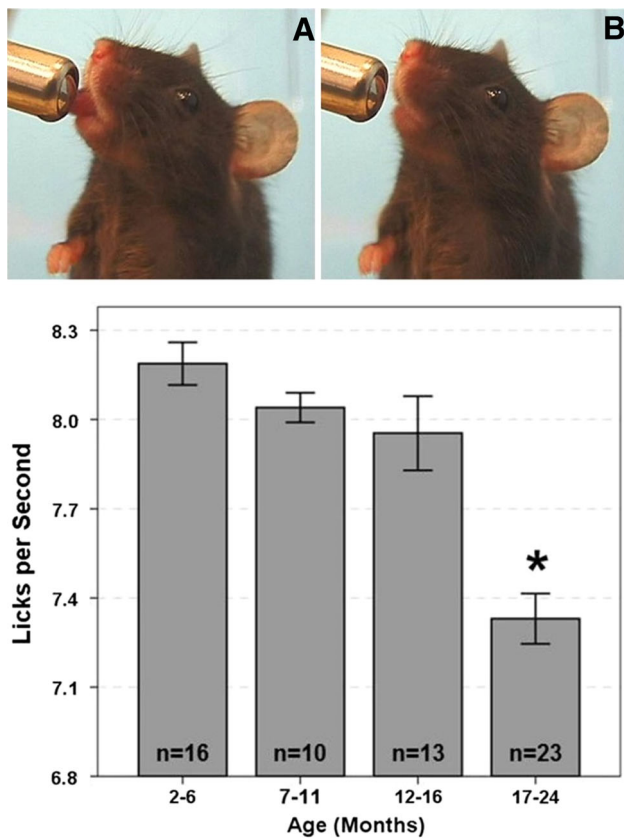


Fig. 1 Lick rate of aging B6 mice. Lick rate (i.e., lick cycles per second) was measured using non-radiographic video recording methods (30 frames per second camcorder with a $\times 0.7$ wide conversion lens) while mice drank room temperature filtered tap water from a sipper tube. Contrasting tongue movements were clearly visible in the video recordings, as shown in Image **a** (maximal tongue protrusion) and Image **b** (tongue retraction). Each lick cycle began with the tongue maximally protruded at the spout, and each subsequent maximal tongue protrusion was counted as an individual lick cycle. As shown in the graph, four age groups of B6 mice were tested to determine the average lick rate across the adult life-span. Lick rate remained relatively stable until 16 months of age and then significantly declined, beginning at 17 months of age. The asterisk represents a significant ($p < 0.05$) difference between age groups; error bars represent ± 1 standard error of the mean (SEM); n = sample size per group

mice sufficiently attenuate the low energy level of the fluoroscope beam, which results in significantly higher contrast resolution than is possible when using conventional high energy fluoroscopes. In addition, The LabScope's 5 cm diameter image intensifier and 6 cm minimum source-to-intensifier distance (SID) provide markedly increased magnification capabilities that are uniquely suited for imaging mice. Additional magnification is achieved using patented technology that enables The LabScope to optically magnify the radiographic image up to 40 times, without altering the SID. Despite these major improvements in small animal fluoroscopy, soft tissue structures (e.g., tongue, velum, posterior pharyngeal wall, and epiglottis) are

not readily visible in this small animal. Therefore, the goal of this study was to quantify bolus flow measures rather than the biomechanics and kinematics of swallowing.

Based on the previously summarized human presbyphagia literature and our preliminary VFSS work with mice, we identified several VFSS swallow metrics that could be reliably quantified in mice for direct comparison with humans, as described in Table 1. We hypothesized that, like healthy aging humans, healthy aging B6 mice would exhibit (1) a migrated anatomical trigger point (i.e., bolus reaching the pyriform sinuses prior to triggering the pharyngeal swallow, indicating a pharyngeal swallow delay), (2) larger bolus sizes to trigger the pharyngeal stage of swallowing, (3) prolonged pharyngeal transit times (PTTs), (4) prolonged esophageal transit times, (5) greater incidence of pharyngeal residue, (6) greater incidence of esophageal residue, and (7) more frequent episodes of laryngeal penetration and aspiration. We also investigated several VFSS metrics that have not yet been reported in the human presbyphagia literature (Table 2), yet are readily quantified in mice [42] and would be feasible for comparative studies between aging mice and people. We hypothesized that aging B6 mice would have longer inter-swallow intervals (ISIs), slower swallow rates, and greater incidences of ineffective primary esophageal swallows and deglutitive inhibition. In addition, we identified several VFSS metrics that are not directly comparable between mice and humans, yet may provide important insights into age-related changes in swallow function in mammals to expand the presbyphagia literature (Table 3). We hypothesized that the VFSS findings would confirm our previous non-radiographic evidence that healthy aging B6 mice have significantly slower lick rates compared to young B6 mice. However, the tongue is not consistently visible during VFSS to permit quantification of lick rate for all mice. In contrast, the jaw is readily visible during VFSS [42]. We hypothesized that jaw cycle rate is identical to tongue cycle rate, which would enable these two measures to be used interchangeably to measure lick rate. We also hypothesized that the lick-swallow ratio would be greater for old versus young B6 mice, indicating that more licks are necessary to trigger pharyngeal swallowing. Finally, we explored potential sex differences for each VFSS metric, with our hypothesis being that dysphagia would be more prevalent in older male than older female mice.

Materials and Methods

Animals

Based on our preliminary findings relative to lick rate using non-radiographic methods, two dichotomous age groups of B6 mice were included in this VFSS investigation: young

Table 1 VFSS metrics that can be directly compared between mice and humans relative to presbyphagia

Swallow metric	Stage of swallowing	Description		
		O	P	E
Swallow trigger point	X	The anatomical location of the pharyngeal swallow trigger point (i.e., where the bolus accumulates in the swallowing mechanism prior to swallowing) is scored using a 3-point scale: 1 (oral cavity), 2 (vallecular space), 3 (pyriform sinuses)		
Bolus Area	X	The size of the bolus (mm^2) that accumulates in lateral view at the “swallow trigger point” immediately before the pharyngeal swallow [42, 62]. A TIFF image is taken of the “rest frame” of bolus accumulation that immediately precedes the swallow response (i.e., visible movement of the bolus through the pharynx into the esophagus). Bolus area (mm^2) in the “rest frame” is measured using NIH ImageJ software, which calculates the area inside a user-defined outlined area on each image. Adjustment for radiologic image magnification is made using a calibration marker placed in the fluoroscopy field of view during testing		
Pharyngeal transit time (PTT)	X	The time (ms) it takes the bolus to be swallowed through the pharynx [42]. The start frame is the “rest frame” that immediately precedes visible transfer of the bolus from the swallow trigger point. The end frame is when the tail of the bolus enters the esophagus. The number of frames between the start and end frames is then divided by 30 fps and converted to milliseconds (ms)		
Esophageal transit time (ETT)	X	The time (ms) it takes the bolus to be swallowed through the esophagus [42]. The start frame is when the bolus tail enters the esophagus (i.e., the PTT end frame). The end frame is when the bolus tail enters the stomach. The number of frames between the start and end frames is then divided by 30 fps and converted to milliseconds (ms)		
Pharyngeal residue	X	The area (mm^2) of post-swallow residue in lateral view in the pharynx, measured using ImageJ software and scaled for magnification using a calibration marker [42]		
Esophageal residue	X	The area (mm^2) of post-swallow residue in lateral view in the esophagus, measured using ImageJ software and scaled for magnification using a calibration marker		
Laryngeal penetration/aspiration	X X	The depth and degree of laryngeal penetration and aspiration, scored using a modified Penetration-Aspiration Scale [63]		

O oral stage, P pharyngeal stage, E esophageal stage

Three to five measures are recorded and averaged for each mouse

Table 2 Translational VFSS metrics that have not been reported for humans with presbyphagia

Swallow metric	Stage of swallowing	Description		
		O	P	E
Inter-swallow interval (ISI)	X X	The time (ms) between two successive, uninterrupted swallows during sequential drinking [42]. The start frame is the “rest frame” that immediately precedes triggering of the pharyngeal swallow. The end frame is the “rest frame” of the next swallow. The number of frames between the two successive swallows is then divided by 30 frames per second (fps) to convert to time (ms). This VFSS metric is an indicator of oral transit time as well as pharyngeal swallow delay		
Swallow rate	X X	The number of swallows occurring during each 2-second episode of uninterrupted (sequential) drinking [42]. This VFSS metric is an indicator of oral transit time as well as pharyngeal swallow delay		
Ineffective primary esophageal swallows	X	The percent of individual pharyngeal swallows that result in incomplete transfer of the bolus through the esophagus into the stomach before the next swallow during sequential drinking. Boluses are scored as 0 (complete transfer) and 1 (incomplete transfer) and then averaged and converted to a percentage		
Deglutitive inhibition	X	The percent of primary esophageal swallows that are abolished by a subsequent pharyngeal swallow during sequential drinking. Boluses are scored as 0 (not abolished) and 1 (abolished) and then averaged and converted to a percentage		

O oral stage, P pharyngeal stage, E esophageal stage

Three to five measures are recorded and averaged for each mouse

(4–7 months of age) and old (18–21 months of age). Our initial intent was to include 8 mice of each sex per age group; however, a smaller cohort of aged B6 mice ($n = 11$;

6 females, 5 males) existed in the colony at the time of this study for comparison with young B6 mice ($n = 16$; 8 females, 8 males). Thus, a total of 27 B6 mice were included

Table 3 VFSS metrics that may not be directly translatable to humans

Swallow metric	Stage of Swallowing	Description		
		O	P	E
Tongue cycle rate	X			
		The number of tongue protrusion/retraction cycles per second (30 frames) during uninterrupted drinking. Each cycle begins with the tongue maximally protruded, and each subsequent maximal tongue protrusion is counted as an individual lick episode (tongue cycle) [36, 37]		
Jaw cycle rate	X			
		The number of jaw open/close (excursion) cycles per second (30 frames) during uninterrupted drinking. Each cycle begins with the jaw maximally opened, and each subsequent maximal jaw excursion is counted as an individual jaw cycle [42]		
Tongue cycles:swallow ratio	X X			
		The number of tongue cycles that occur during each ISI (i.e., between two successive, uninterrupted swallows) [42]. This VFSS metric is an indicator of oral transit time as well as pharyngeal swallow delay		
Jaw cycles:swallow ratio	X X			
		The number of jaw cycles that occur during each ISI (i.e., between two successive, uninterrupted swallows) [42]. This VFSS metric is an indicator of oral transit time as well as pharyngeal swallow delay		

O oral stage, P pharyngeal stage, E esophageal stage

Three to five measures are recorded and averaged for each mouse

in this study, which was approved by the Institutional Animal Care and Use Committee (IACUC) of the University of Missouri. All mice were offspring from a B6 colony established at the University of Missouri from B6 sibling pairs purchased from The Jackson Laboratory (Bar Harbor, ME). The colony was maintained by mating male colony offspring with age-matched (~6 week old) B6 females purchased from The Jackson Laboratory. Once a year, new B6 sibling breeder pairs were purchased from The Jackson Laboratory to prevent genetic drift from the B6 founder line. Offspring were weaned at 21–24 days of age and group housed based on sex, with 3–5 mice per cage. Mice were housed in a standard 12:12 light/dark cycle facility with controlled temperature (64–79 °F) and humidity (30–70 %) conditions. Unlimited access to food and water was provided, except during a single overnight water restriction period prior to VFSS testing, as described below. In an effort to minimize aggressive behaviors, which are common among aging mice [43–45], we added the following enrichment materials weekly to each cage: two hiding options (hut and paper tube), a nestlet (split in half), dental treats (e.g., pieces of dried tree branches), and food treats (e.g., nut and seed mix) scattered on top of the fresh bedding material. In addition, a small piece of lightly soiled nesting material was transferred each week into the new home cage, which has been shown to reduce stress-related aggressive behaviors in mice [46]. Daily checks by research and veterinary staff ensured that all mice remained healthy and harmonious throughout the study in this enriched group housing environment.

Videofluoroscopic Swallow Study (VFSS) Protocol

All mice underwent VFSS testing in accordance with a recently established protocol in our lab [42]. Young B6

mice were tested once between 4 and 7 months of age, whereas aged B6 mice were tested once between 18 and 21 months of age. Multiple VFSS tests were not conducted for each mouse because the effects of repeated whole body radiation on mice are currently unknown and could potentially confound outcomes.

Beginning 2 weeks prior to VFSS testing, mice were subjected to a behavioral conditioning program that entailed two components: (1) a solution of 3 % chocolate-flavored water (i.e., without contrast agent added) was offered in the home cage 1–2 times per week for 1–2 h at a time to assure familiarity and acceptance of the chocolate-flavored VFSS test solution, and (2) a custom-designed VFSS test chamber (Fig. 2) was placed overnight in each home cage once a week to assure familiarity of the VFSS testing environment (Fig. 3). The night before VFSS testing, mice were subjected to an overnight (~16 h) water restriction to induce thirst. At the start of the water restriction, mice were transferred to a fresh home cage and provided with free access to standard rodent food pellets; water was withheld. A VFSS test chamber was placed on the floor of each home cage to provide a final overnight acclimation period to the test environment. The following morning, each test chamber was rinsed with water (to remove soiled bedding material), dried with a paper towel, and returned to the home cage in preparation for VFSS testing.

A thin liquid oral contrast agent was prepared according to our standard protocol using a 50 % solution of stock iohexol (350 mg iodine per mL) flavored with chocolate syrup [42], as shown in Table 4. The test solution was administered at room temperature and used within 4 h of preparation. We have found that longer storage durations alter palatability and result in avoidance behaviors by mice.

Mice underwent VFSS testing one at a time in the same test chamber that was used during the overnight water

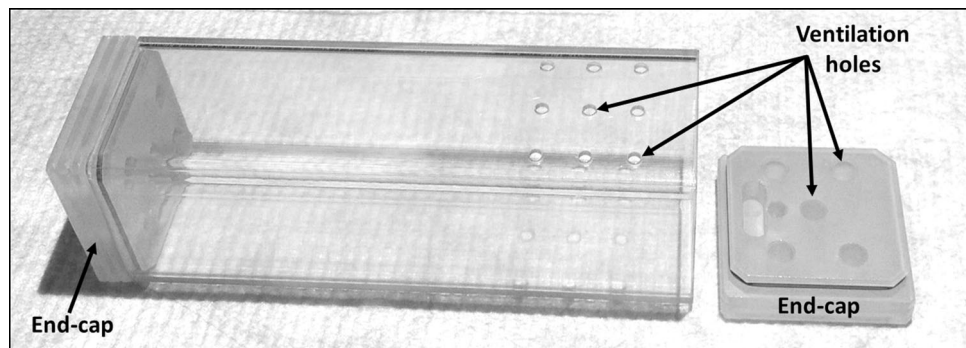


Fig. 2 VFSS test chamber. Each polycarbonate test chamber consisted of a 5 cm square diameter tube that was 15 cm long and fitted with two removable end-caps. Polycarbonate material was used

because it is extremely durable, translucent, radiolucent, and autoclavable. Ventilation holes in the chamber ceiling and end-caps permitted sufficient air flow during testing

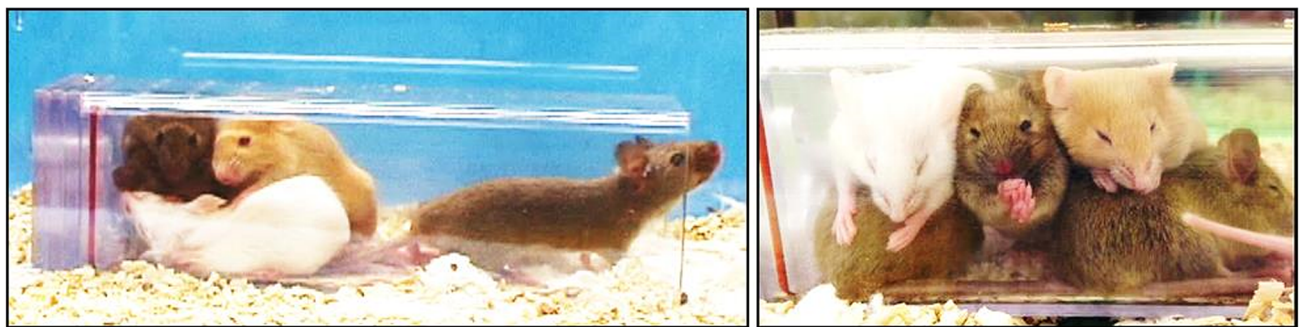


Fig. 3 Overnight acclimation period. One test chamber was placed in each home cage overnight for mice to explore. *Left* Only one end of the chamber was closed by an end-cap; the other end remained open

to allow mice to freely enter and exit. *Right* The following morning, most mice were found sleeping in huddled fashion deep within the chamber, indicating acceptance of the test environment

Table 4 Oral contrast recipe for thin liquid

Ingredients	Volume (mL)
Chocolate syrup	3
Filtered tap water	12
Omnipaque (350 mgI/mL) ^a	15
Final volume	30

^a GE Healthcare

restriction period. Mice were easily coaxed to enter the chamber by strategically placing the chamber opening in front of a mouse inside the home cage, or by suspending a mouse by the tail over the chamber opening. The mouse was then enclosed in the chamber by simply attaching the 2nd end-cap. The test chamber prevented escape while creating a quiet, low anxiety environment that restricted extraneous exploratory behaviors. Immediately after enclosing the mouse, the test chamber was positioned on a remote-controlled scissor lift table within the c-arm portion of The LabScope fluoroscopy system (Fig. 4). A webcam positioned above the chamber provided real-time viewing of the mouse at all times. VFSS testing was performed in

the lateral (horizontal) plane while remotely adjusting the lift table as needed to maintain the swallowing mechanism of each mouse in the fluoroscopy field of view. Liquid contrast solution was delivered into a bowl (i.e., peg-bowl) using a syringe delivery system (Fig. 5). To minimize radiation exposure, the fluoroscopy machine was activated only when the mouse approached the bowl (as viewed via webcam) and was immediately deactivated each time the mouse turned away. Once engaged in drinking, mice remained remarkably self-stabilized for several seconds at a time, resulting in minimal movement artifact.

The markedly greater magnification of The LabScope (compared to high energy fluoroscopy systems) necessitated two test positions to assess the entire swallowing mechanism of mice (Fig. 6). Position 1 permitted visualization of the entire head and proximal thoracic region to assess the oral and pharyngeal stages of swallowing. Position 2 permitted visualization of the proximal thoracic region to the gastroesophageal (GE) junction and stomach to assess the esophageal stage of swallowing. A radiopaque marker of known dimensions was placed in the fluoroscopy field of view (affixed to the image intensifier) for calibration purposes. Position 1 was tested first, which typically

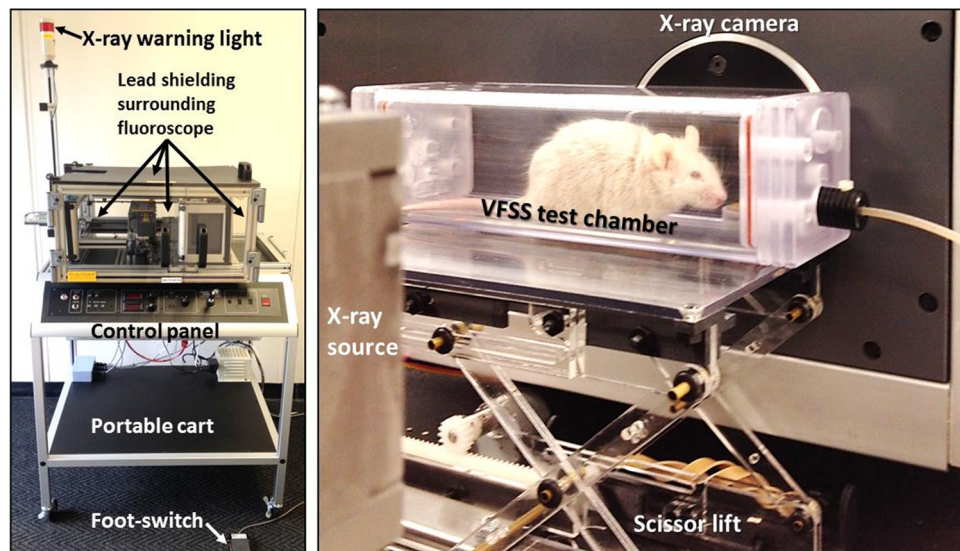


Fig. 4 The LabScope fluoroscopy system. A miniature low energy fluoroscopy system (i.e., The LabScope, Glenbrook Technologies) was customized for VFSS testing of mice. *Left* Front view of The LabScope showing labeled components. Lead acrylic shielding surrounds the system to block scattered X-ray photons, which eliminates the need for personal shielding (e.g., lead apron, thyroid

shield, and eyeglasses). *Right* VFSS test chamber with a mouse positioned in lateral view within the fluoroscope. Radiation safety is further improved by using a motorized scissor lift table that permits remote positioning of the test chamber from a distance of 1 m (or further, if needed)

entailed ~15 s of drinking with minimal to no interruption. Using the remote-controlled scissor lift, the mouse was then immediately moved to Position 2, which entailed ~15 additional seconds of drinking. This approach resulted in each mouse typically receiving less than 1 min of radiation exposure during the entire procedure. Video recordings of each test were digitally captured as AVI files at 30 frames per second (fps).

Video Analysis

All videos were initially viewed by the first author (TEL) to identify and analyze five separate 2-second episodes of uninterrupted drinking per mouse for each fluoroscopy position (i.e., Position 1 and Position 2). The ten 2-second video clips per mouse were analyzed frame-by-frame using video editing software (Pinnacle Systems, Inc., Mountain View, CA) to quantify 3–5 measures of the 15 swallow metrics included in this study, as described in Tables 1, 2, and 3. This criterion was based on published VFSS studies with mice [42] and rats [47] and non-radiographic swallow studies with mice [36, 37] showing that 3–5 measures per swallow metric are sufficient for statistical analysis. A second reviewer (MJA or MDK) independently re-analyzed each 2-second video clip in blinded fashion, using only the starting frames identified by the first reviewer. All value discrepancies were subjected to group consensus to resolve reviewer error. This approach resulted in 100 % reliability between all reviewers for each of the 15 VFSS metrics.

Rheologic Measurements

Viscosity of the liquid test solution was measured at room temperature (25 °C) using a cone and plate viscometer (HAAKE™ RheoStress™ 100 5 N cm viscometer with a 35 mm diameter, 4° cone). The viscometer's software (HAAKE RheoWin 1.97) was programmed to run at a shear rate of 50.00 s⁻¹, which is the standard shear rate for the National Dysphagia Diet [48]. Three samples were freshly made and tested separately after transient vortexing before use. The density of each sample was determined by weighing a 1 mL volume and converting to kg/m³. Approximately 1.5 mL of each sample was pipetted onto the viscometer plate, and the cone-plate gap was set to 0.138 mm. Data collection began when the torque gradient (i.e., viscosity equilibrium) fell below 5 mPa. Twenty apparent viscosity data points were recorded for each sample. These 20 data points were automatically averaged and reduced to a single data point per sample, reported in centipoise (cP). The averaged viscosity values for each of the three samples were subsequently averaged to produce a single viscosity measurement for the test solution.

Statistical Analysis

Statistical analysis was generated using SAS/STAT software (version 9.3 of the SAS System for Windows, copyright 2002–2010 by SAS Institute Inc., Cary, NC). A repeated measures ANOVA (factors age and sex) was performed on all continuous variables (i.e., swallow

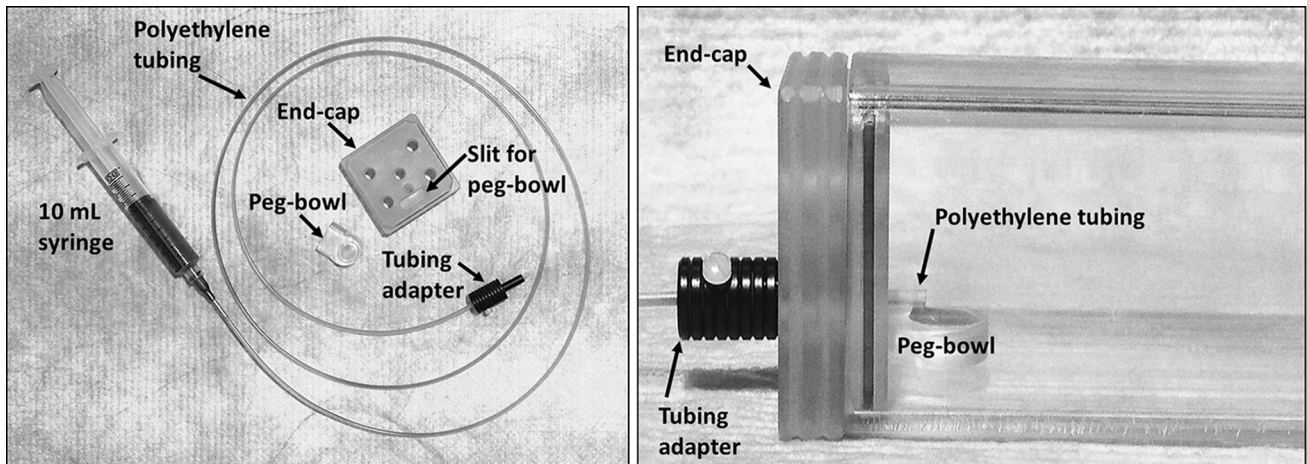


Fig. 5 Syringe delivery system for liquid contrast solution. The liquid contrast solution (i.e., chocolate-flavored iohexol) is administered into a peg-bowl during VFSS using a custom syringe delivery system. *Left* Labeled components of the syringe delivery system.

Right Assembled components with a VFSS test chamber. This system permits controlled delivery of liquid from a distance of 1 m (or further, if needed) to improve radiation safety during VFSS

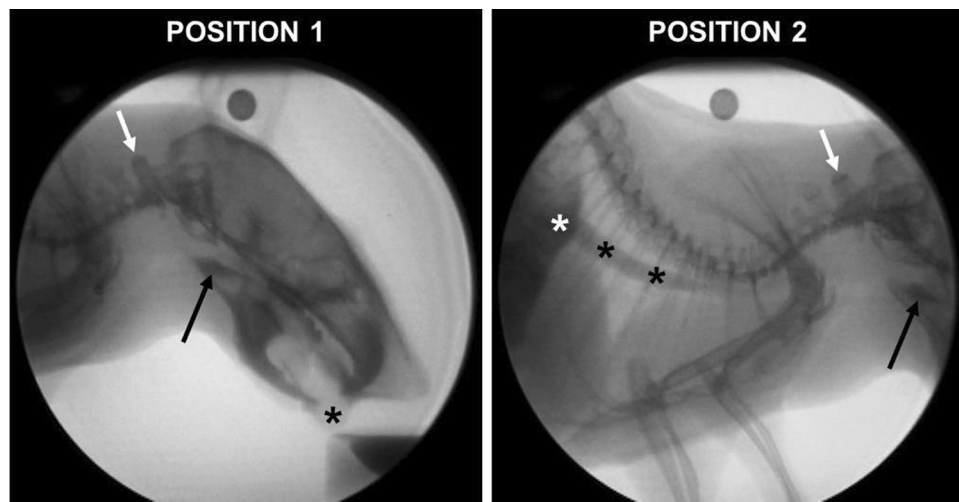


Fig. 6 VFSS test positions. Lateral radiographic images of a mouse, obtained using a low energy fluoroscopy system (i.e., The LabScope). The high fluoroscopic magnification necessitates two test positions to visualize the entire swallowing mechanism. *Left (Position 1)* The entire head and proximal thoracic region are visible in the fluoroscopy field of view, with the swallow trigger point (i.e., vallecular space; black arrow) positioned in the center. The tongue (black asterisk) is visible as the mouse drinks from the bowl. *Right (Position 2)* The

fluoroscopy field of view spans from the swallow trigger point (black arrow) to the stomach (white asterisk). Note the bolus (black asterisks) passing through the distal esophagus as the vallecular space (black arrow) fills in preparation for the next swallow. White arrows in both frames: 2nd cervical vertebra; black circles centered at the top of each field of view: radiopaque marker for scaling the fluoroscopic image magnification

metrics) for which 3–5 measurements were obtained: PTT, esophageal transit time (ETT), pharyngeal residue, esophageal residue, ISI, swallow rate, tongue cycle rate, jaw cycle rate, tongue cycle-swallow ratio, jaw cycle-swallow ratio. A two-way ANOVA (factors age and sex) was used for bolus area because there was only one measurement (i.e., average bolus area) for each mouse. The assumptions for ANOVA were first examined via exploratory analysis and residual plots. One-sided post hoc tests were used

because all research hypotheses for this study were directional. When the factor sex was not significant, the parsimonious single factor (age) model was fit to the data. When non-normality of the model residuals was present, normalizing transformations of responses were investigated using the Box–Cox class of power transformations. The ANOVA model was then run for the transformed data, followed by residual diagnostics and appropriate one-sided post hoc tests. Finally, when residuals did not pass the test of

normality and normalizing transformations were not successful, the data were analyzed using non-parametric methods, specifically the one-sided Wilcoxon rank sum test. Two of the variables (primary esophageal swallows and esophageal swallow inhibition) were dichotomous (0 or 1) and were analyzed using the generalized linear model (factors age and sex), data distribution binomial, and logit link function, followed by one-sided post hoc tests when warranted. A *p* value of <0.05 defined significance for all statistical analyses. For non-significant findings, power calculations were conducted to determine the required total sample size for achieving 80 % power of detection of a significant difference, using the one-sided two-sample *t* test.

Results

All mice remained healthy throughout this study, without developing overt signs of disease conditions. Initial statistical analysis for each swallow metric revealed that the factor sex was not significant. Therefore, the results presented here relate only to the age factor. Results are grouped according to the VFSS metrics previously defined in Tables 1, 2, and 3. The combined results are shown in Table 5.

Table 1 metrics: VFSS swallow metrics that can be reliably quantified in mice for direct comparison with humans

Of the seven VFSS metrics defined in Table 1, three were significantly different between young and old mice: bolus area ($F = 5.17, p = 0.0318$), PTT ($F = 4.82, p = 0.0376$), and ETT ($F = 11.84, p = 0.0222$). For bolus area and PTT, one-sided *t*-tests revealed that old mice have significantly larger bolus areas ($t = 2.27, p = 0.0156$; Fig. 7a) and significantly longer PTTs ($t = 2.20, p = 0.0188$; Fig. 7b) than young mice. PTT residuals showed some departure from normality and transformations were not an effective remedy. Therefore, the non-parametric test (Wilcoxon rank sum) was run, which confirmed the previous results of a significant age effect for PTT ($Z = 2.39, p = 0.0083$). For ETT, a normalizing transformation (Box–Cox) was used because non-normality was exhibited. A one-sided *t*-test showed that ETT was significantly longer for old compared to young mice ($t = 3.45, p = 0.0011$; Fig. 7c).

The anatomical location of the swallow trigger point was invariably the vallecular space for all mice, regardless of age. In addition, there were no instances of laryngeal penetration/aspiration, pharyngeal residue, or esophageal residue. Since all observed values were identical, statistics on variability could not be calculated and we were unable to perform any testing or inferential methods for these four variables.

Table 2 metrics: VFSS metrics that have not yet been reported in the human presbyphagia literature, yet are readily quantified in mice and would be feasible for comparative studies between aging mice and people

Of the four VFSS metrics defined in Table 2, only one was significantly different between young and old mice: ineffective primary esophageal swallows ($X^2 = 3.05, p = 0.0808$). A one-sided *t* test showed that old mice had a significantly higher percentage of ineffective primary esophageal swallows than young mice ($z = 1.74, p = 0.0405$), as shown in Fig. 7d. No significant age effect was identified for inter-swallow-interval ($p = 0.4006$), swallow rate ($p = 0.2024$), and deglutitive inhibition ($p = 0.1867$).

Table 3 metrics: VFSS metrics that may not be directly compared between mice and humans, yet may provide important insights into age-related changes in swallow function in mammals to expand the presbyphagia literature

Of the four VFSS metrics defined in Table 3, only two were significantly different between young and old mice: tongue cycle rate ($F = 10.46, p = 0.0034$) and jaw cycle rate ($F = 11.88, p = 0.0020$). One-sided *t* tests showed that old mice had significantly slower tongue cycle ($t = 3.23, p = 0.0017$) and jaw cycle ($t = 3.45, p = 0.0010$) rates compared to young mice (Fig. 7e). The residuals for jaw cycle rate showed slight departure from normality. Therefore, the non-parametric test (Wilcoxon rank sum) was run, which confirmed the age effect ($Z = 3.0631, p = 0.0011$). No significant age effects were identified for tongue cycle–swallow ratio ($p = 0.6358$) and jaw cycle–swallow ratio ($p = 0.2939$).

In several cases, the tongue was not clearly visible during VFSS to permit quantification of tongue cycle rate. However, jaw cycle rate was consistently quantifiable for all mice. Every time both observations (i.e., tongue and jaw cycle rates) were quantifiable from the same mouse, they were identical (Fig. 7e), suggesting that either anatomical structure (tongue or jaw) can be used to measure lick rate.

Power calculations were performed for all non-significant findings. We determined that increasing the sample size to 16 mice per age group (i.e., 32 mice total) would yield statistical significance at 80 % power, using the two-sample *t* test procedure ($\alpha = 0.05$, one-sided). Greater than 400 mice per group would be required for all other non-significant VFSS metrics, which is not feasible to consider for future studies. These results are summarized in Table 5.

Rheologic Measurements

The average density of the iohexol test solution at 25 °C was 1187.5 kg/m³. The average viscosity at 25 °C and a

Table 5 VFSS metrics

VFSS metric	<i>p</i> value	Sample size calculation
Swallow trigger point	n/a	
Bolus area	<i>0.0156</i>	
Pharyngeal transit time (PTT)	<i>0.0188</i>	
Esophageal transit time (ETT)	<i>0.0011</i>	
Pharyngeal residue	n/a	
Esophageal residue	n/a	
Laryngeal penetration/aspiration	n/a	
Inter-swallow Interval	0.4006	408
Swallow rate	0.2024	696
Ineffective primary esophageal swallows	<i>0.0405</i>	
Deglutitive inhibition	0.1867	32
Tongue cycle rate	<i>0.0017</i>	
Jaw cycle rate	<i>0.0010</i>	
Tongue cycle-swallow ratio	0.6358	1842
Jaw cycle-swallow ratio	0.2939	5470

Italicized text indicates statistical significance; n/a indicates *p* values were not applicable because there was no difference in the data obtained from both groups. Total sample size calculations are shown for all non-significant findings

shear rate of 50 s⁻¹ was 5.41 cP. Data for each of the three test samples are shown in Table 6.

Discussion

In this study, we examined age-related differences in the swallow function of young (4–7 months) versus old (18–21 months) B6 mice using a murine videofluoroscopy protocol that was recently developed in our lab [42]. We hypothesized that healthy aging B6 mice would develop age-related changes in the oral, pharyngeal, and esophageal stages of swallowing similar to presbyphagia in humans. To test this hypothesis, we quantified 15 VFSS swallow metrics that were divided into three discrete categories: (1) metrics previously used to detect presbyphagia in humans, (2) metrics that have not yet been reported in the human presbyphagia literature, yet are readily quantified in mice and would be feasible for comparative studies between aging mice and humans, and (3) metrics that are not directly comparable between mice and humans, yet may provide important insights into age-related changes in swallow function in mammals to expand the presbyphagia literature. Our goal was to identify robust VFSS biomarkers that can detect subtle but clinically important changes in the swallow function of aging mice using small sample sizes. Results showed that 6 of the 15 metrics were significantly different for old compared to young B6 mice. Thus, this study provides novel evidence that healthy aging B6 mice indeed develop age-related changes in swallow function, thereby providing initial validation of B6 mice as a suitable translational murine model of presbyphagia.

Three of the six impaired VFSS metrics (i.e., bolus area, PTT, and ETT) closely resembled the clinical signs of presbyphagia reported in studies of primary aging humans: significantly longer pharyngeal [1, 4, 6, 10, 11] and esophageal [12–14] transit times and significantly larger bolus volumes to trigger the pharyngeal swallow response [15]. One of the six impaired metrics (i.e., ineffective primary esophageal swallows) has not yet been investigated in primary aging humans. This finding suggests a potential role for this VFSS metric in detecting age-related esophageal dysfunction in humans. However, a caveat to consider is the esophagus of adult mice is comprised entirely of striated muscle [49]; therefore, species differences in the esophagus must be taken into consideration. Two of the impaired metrics pertained to lick rate (i.e., tongue and jaw cycles per second), which is not directly comparable to humans. Whereas licking behaviors in mice are essential to life as a means of acquiring nutrition [38, 50], ingestion of liquids by humans is accomplished by cup or straw drinking. Although these species-specific oral behaviors look quite different, they both utilize the tongue, jaw, and other structures of the oral cavity to serve a common purpose of nutritive ingestion; therefore, they are presumed to utilize common neural substrates. We propose that investigating the pathological mechanisms responsible for slower lick rates in aging B6 mice may provide translational insights into the deterioration of the oral stage of swallowing in healthy aging humans.

No episodes of laryngeal penetration or aspiration were observed for any mice during this study, regardless of age. It is possible the contrast density of the 50 % iohexol oral contrast agent was not adequate for identifying trace

Fig. 7 Evidence of presbyphagia in aging B6 Mice. **a** Bolus area was significantly larger for old compared to young mice. Pharyngeal (**b**) and esophageal (**c**) transit times were significantly longer for old compared to young mice. **d** Old mice had a significantly higher proportion of ineffective esophageal swallows compared to young mice. **e** Old mice licked significantly slower than young mice. The number of tongue versus jaw cycles per second was identical for each mouse. Asterisks represent a significant ($p < 0.05$) difference between age groups; error bars represent ± 1 standard error of the mean (SEM); n = sample size per age group

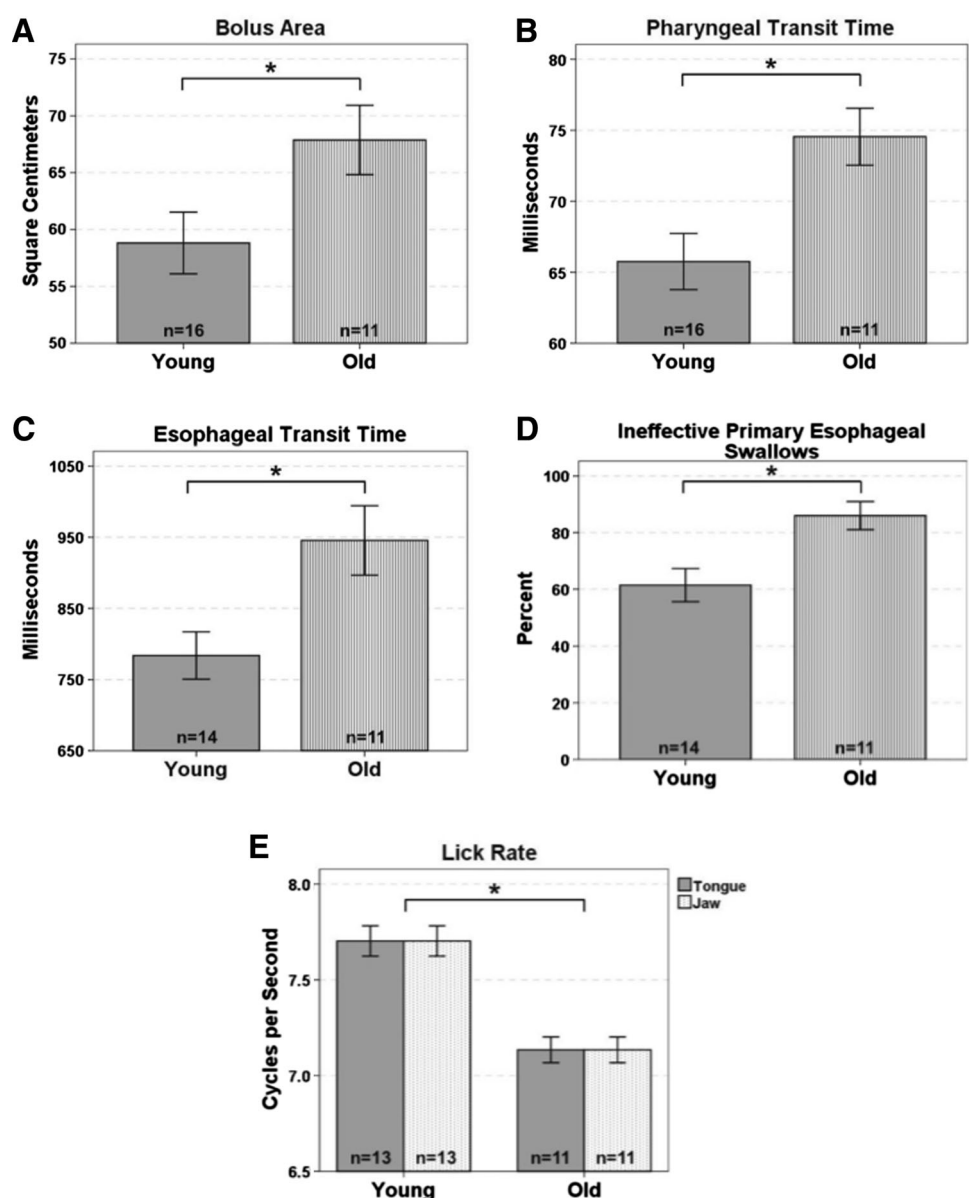


Table 6 Rheologic measurements

Sample	Density (kg/m ³)	Viscosity (cP)
1	1183.3	5.58
2	1194.9	5.23
3	1184.4	5.41
Average	1187.5	5.41

All values were recorded at 25 °C. Viscosity was measured at a shear rate of 50 s⁻¹

penetration/aspiration. However, this contrast density did provide sufficient visualization and quantification of numerous bolus flow events in mice during videofluoroscopy, using a low energy system (The LabScope, Glenbrook

Technologies) that was specifically designed for use with mice and other small rodents. A more likely explanation for the unexpected absence of laryngeal penetration/aspiration events in aging mice may be the anatomical differences in the swallowing mechanism between mice and humans. We have studied the oral, pharyngeal, and laryngeal anatomy of hundreds of mice over the past year using a transoral laryngoscopy procedure developed in our lab [51]. In all cases, the velum and epiglottis were tightly coupled during rest breathing through the nose, and the glottis could be visualized only after insertion of a miniature laryngoscope between the velum and epiglottis, as shown in Fig. 8. Thereafter, mice transitioned to an oral mode of breathing, as has been reported in other studies investigating the effects of nasal occlusion in mice [52, 53].

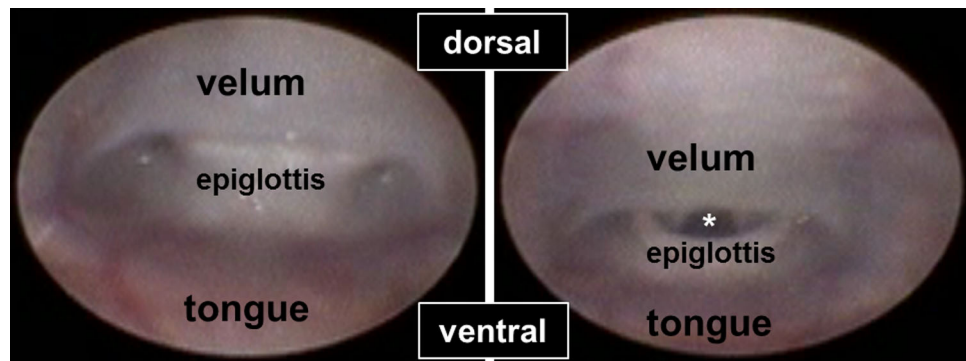
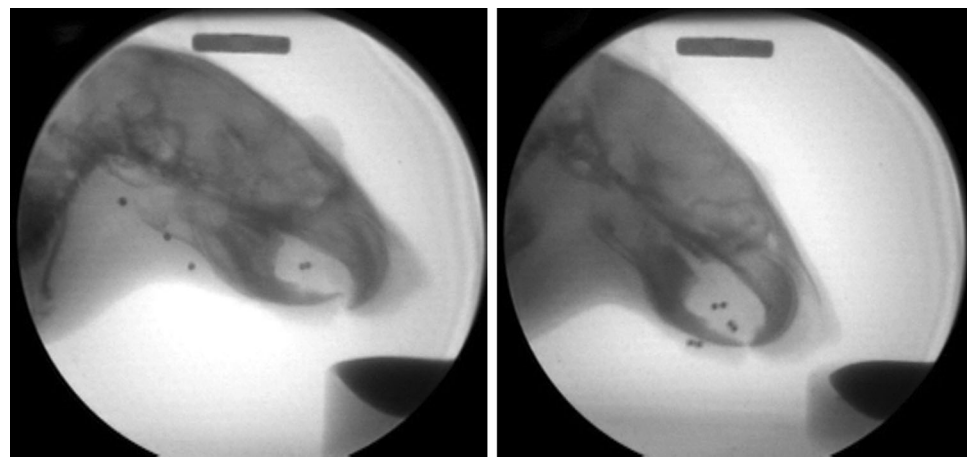


Fig. 8 Anatomical differences in the murine larynx. These images were obtained using a transoral murine laryngoscopy procedure developed in our lab. *Left* The velum and epiglottis are tightly approximated during rest breathing in mice, which prevents

visualization of the vocal folds during transoral laryngoscopy. *Right* The glottis (white asterisk) is visualized only after mechanical separation of the velum and glottis using a miniature laryngoscope

Fig. 9 Radiopaque marker implants. Representative radiographic images of mice demonstrating successful implantation of radiopaque markers (0.05 mm tungsten carbide balls) into various soft tissue structures of the swallowing mechanism



In other words, mice are preferential nasal breathers whose larynx is inherently protected from the normal path of bolus flow during swallowing. This major structural difference in the swallowing mechanism of mice suggests that laryngeal penetration and aspiration may not be a clinical sign of dysphagia in any mouse model. However, as suggested by this study, the swallowing mechanism of these two species must be sufficiently similar to produce common signs of swallowing dysfunction as a consequence of aging.

A major limitation of this study was that it included only liquid trials. The apparent viscosity of the test solution was 5.41 cP, which falls within the wide range for thin liquids (1–50 cP) established by the National Dysphagia Diet; however, it just barely exceeds the narrow range (1–5 cP) [48]. Additionally, the average density of the test solution was 1187.5 kg/m³, which is slightly above the density of pure water (1000 kg/m³). We recognize that VFSS with humans includes several consistencies of foods and liquids,

and dysphagia is often most apparent when swallowing very thin liquids and dry solid foods [54, 55]. Therefore, we are in the process of expanding our murine VFSS protocol by developing species-specific recipes for additional consistencies that may facilitate detection and quantification of dysphagia in murine disease models. Examples include thinner liquids (i.e., closer to 1 cP and 1000 kg/m³ to more closely resemble water) and dry foods that require mastication.

Although hundreds of murine (mouse and rat) models are commercially available to study human diseases, only four have been investigated relative to dysphagia: a mouse model of ALS [36, 37] and rat models of stroke [56], Parkinson's disease [47, 57–59], and primary aging [47]. Aside from our work, only one other published murine study has utilized VFSS [47]. The study entailed offering a mixture of peanut butter and barium (resembling a pudding consistency) to three different groups of rats: young controls ($n = 7$), young rats with experimentally induced

Parkinson disease ($n = 8$), and healthy old rats ($n = 7$). However, results were limited because the rats did not remain in the videofluoroscopic field of view during testing. Moreover, the VFSS results from aging rats cannot be directly compared with our results from aging mice because the studies did not investigate the same VFSS metrics and did not utilize similar consistencies for the test items. We expect this major limitation may be overcome in future studies by utilizing a common murine VFSS protocol in research, which would facilitate identification of objective measures (biomarkers) of swallow function/dysfunction that could be directly compared between species.

Additional limitations of this study included two technological barriers. First, we recently showed that swallowing in mice is approximately 10 times faster than humans [42], which necessitates the use of much higher video recording frame rates (likely over 100 fps) to improve the diagnostic potential of VFSS in future studies with this small animal. Second, it is difficult to discern soft tissue anatomy of mice under fluoroscopy to permit assessment of the biomechanics of swallowing for comparison with humans. We have been exploring the use of implantable radiopaque markers to permit visualization of various soft tissue structures of the swallowing mechanism, such as the tongue, soft palate, pharynx, larynx, and proximal esophagus (Fig. 9). A similar approach has been successfully used for many years to study the biomechanics of swallowing in infant pigs [60, 61]. We envision overcoming this barrier will open the possibility of automated quantification of biomechanics during murine VFSS rather than relying predominantly on manual calculations of bolus flow characteristics.

A key distinction addressed by this study is whether presbyphagia is a sign of healthy aging (i.e., primary aging) versus an early indicator of an age-related disease that has not yet been diagnosed but is associated with dysphagia. B6 mice are an ideal animal model to elucidate this distinction because they have one of the longest life-spans of mice, often surviving more than 24 months without developing tumors or diseases [33]. As expected, none of the aging B6 mice in this study developed signs of illness or disease, despite showing age-related changes in swallow function. This finding further validates B6 mice as a translational model of primary aging and provides strong rationale for using this strain in future studies to investigate the molecular mechanisms driving presbyphagia.

Acknowledgments We graciously thank past members of the Lever Lab who contributed to preliminary data collection using non-radiographic lick rate methods (Danarae Aleman, Laura Powell, and Andries Ferreira). We also acknowledge Roderic Schlotzhauer from the University of Missouri Physics Machine Shop for design input and fabrication of the VFSS test chambers that were essential to this study. We sincerely thank Dr. Fu-Hung Hsieh's lab at the University

of Missouri Department of Bioengineering for assistance in gathering rheological data. Our highest gratitude extends to Dr. Grace Pavlath (Emory University), who facilitated our acquisition of the fluoroscope used to collect data for this study. This study was funded by NIH/NIDCD (R03DC010895, TE Lever), NIH/NINDS (R21N5084870-01, GK Pavlath), Otolaryngology – Head and Neck Surgery start-up funds (TE Lever), MU PRIME Fund (TE Lever), Mizzou Advantage (TE Lever), and the MU Center on Aging (TE Lever).

Conflict of interest The authors declare that they have no conflict of interest.

References

1. Robbins J, Hamilton JW, Lof GL, Kempster GB. Oropharyngeal swallowing in normal adults of different ages. *Gastroenterology*. 1992;103:823–9.
2. Ney DM, Weiss JM, Kind AJ, Robbins J. Senescent swallowing: impact, strategies, and interventions. *Nutr Clin Pract*. 2009;24: 395–413.
3. Robbins J, Bridges AD, Taylor A. Oral, pharyngeal and esophageal motor function in aging. *GI Motility online*. Nature.com. London: Macmillan Publishers Limited; 2006.
4. Cook IJ, Weltman MD, Wallace K, Shaw DW, McKay E, Smart RC, Butler SP. Influence of aging on oral-pharyngeal bolus transit and clearance during swallowing: scintigraphic study. *Am J Physiol*. 1994;266:G972–7.
5. Leslie P, Drinnan MJ, Ford GA, Wilson JA. Swallow respiratory patterns and aging: presbyphagia or dysphagia? *J Gerontol A*. 2005;60:391–5.
6. Tracy JF, Logemann JA, Kahrilas PJ, Jacob P, Kobara M, Krugler C. Preliminary observations on the effects of age on oropharyngeal deglutition. *Dysphagia*. 1989;4:90–4.
7. Bisch EM, Logemann JA, Rademaker AW, Kahrilas PJ, Lazarus CL. Pharyngeal effects of bolus volume, viscosity, and temperature in patients with dysphagia resulting from neurologic impairment and in normal subjects. *J Speech Hear Res*. 1994;37:1041–59.
8. Lazarus CL, Logemann JA, Rademaker AW, Kahrilas PJ, Pajak T, Lazar R, Halper A. Effects of bolus volume, viscosity, and repeated swallows in nonstroke subjects and stroke patients. *Arch Phys Med Rehabil*. 1993;74:1066–70.
9. Logemann JA, Kahrilas PJ, Cheng J, Pauloski BR, Gibbons PJ, Rademaker AW, Lin S. Closure mechanisms of laryngeal vestibule during swallow. *Am J Physiol*. 1992;262:G338–44.
10. Ekberg O, Feinberg MJ. Altered swallowing function in elderly patients without dysphagia: radiologic findings in 56 cases. *AJR Am J Roentgenol*. 1991;156:1181–4.
11. Yoshikawa M, Yoshida M, Nagasaki T, Tanimoto K, Tsuga K, Akagawa Y, Komatsu T. Aspects of swallowing in healthy dentate elderly persons older than 80 years. *J Gerontol A*. 2005;60:506–9.
12. Zboralske FF, Amberg JR, Soergel KH. Presbyesophagus: cineradiographic manifestations. *Radiology*. 1964;82:463–7.
13. Aly YA, Abdel-Aty H. Normal oesophageal transit time on digital radiography. *Clin Radiol*. 1999;54:545–9.
14. Soergel KH, Zboralske FF, Amberg JR. Presbyesophagus: esophageal motility in nonagenarians. *J Clin Invest*. 1964;43: 1472–9.
15. Shaker R, Ren J, Zamir Z, Sarna A, Liu J, Sui Z. Effect of aging, position, and temperature on the threshold volume triggering pharyngeal swallows. *Gastroenterology*. 1994;107:396–402.

16. Humbert IA, Fitzgerald ME, McLaren DG, Johnson S, Porcaro E, Kosmatka K, Hind J, Robbins J. Neurophysiology of swallowing: effects of age and bolus type. *Neuroimage*. 2009;44: 982–91.
17. Butler SG, Maslan J, Stuart A, Leng X, Wilhelm E, Lintzenich CR, Williamson J, Kritchevsky SB. Factors influencing bolus dwell times in healthy older adults assessed endoscopically. *Laryngoscope*. 2011;121:2526–34.
18. Butler SG, Stuart A, Kemp S. Flexible endoscopic evaluation of swallowing in healthy young and older adults. *Ann Otol Rhinol Laryngol*. 2009;118:99–106.
19. Butler SG, Stuart A, Markley L, Rees C. Penetration and aspiration in healthy older adults as assessed during endoscopic evaluation of swallowing. *Ann Otol Rhinol Laryngol*. 2009;118:190–8.
20. Robbins J, Coyle J, Rosenbek J, Roecker E, Wood J. Differentiation of normal and abnormal airway protection during swallowing using the penetration–aspiration scale. *Dysphagia*. 1999;14:228–32.
21. Grishaw EK, Ott DJ, Frederick MG, Gelfand DW, Chen MY. Functional abnormalities of the esophagus: a prospective analysis of radiographic findings relative to age and symptoms. *AJR Am J Roentgenol*. 1996;167:719–23.
22. Kays S, Robbins J. Effects of sensorimotor exercise on swallowing outcomes relative to age and age-related disease. *Semin Speech Lang*. 2006;27:245–59.
23. Humbert IA, Robbins J. Dysphagia in the elderly. *Phys Med Rehabil Clin N Am*. 2008;19:853–66.
24. Bureau USC: Statistical Abstract of the United States: 2012. 2012.
25. Howden CW. Management of acid-related disorders in patients with dysphagia. *Am J Med*. 2004;117(Suppl 5A):44S–8S.
26. Seshamani M, Kashima M. Age-related swallowing changes. 5th ed. Philadelphia: Mosby-Elsevier; 2010.
27. Roy N, Stemple J, Merrill RM, Thomas L. Epidemiology of voice disorders in the elderly: preliminary findings. *Laryngoscope*. 2007;117:628–33.
28. Bult CJ, Eppig JT, Blake JA, Kadin JA, Richardson JE. The mouse genome database: genotypes, phenotypes, and models of human disease. *Nucleic Acids Res*. 2013;41:D885–91.
29. Battey J, Peterson J. Model organisms for biomedical research, trans-NIH mouse initiatives. 2014.
30. Abdelkafy WM, Smith JQ, Henriquez OA, Golub JS, Xu J, Rojas M, Brigham KL, Johns MM. Age-related changes in the murine larynx: initial validation of a mouse model. *Ann Otol Rhinol Laryngol*. 2007;116:618–22.
31. Laboratory J. Genotyping protocol for SOD. 2013: from http://jaxmice.jax.org/pub-cgi/protocols/protocols.sh?objtype=protocol&protocol_id=523, 2009.
32. Jackson L. Genotyping protocol for SOD. 2013: from http://jaxmice.jax.org/pub-cgi/protocols/protocols.sh?objtype=protocol&protocol_id=523, 2009.
33. Laboratory TJ. JAX Mice Database. <http://jaxmice.jax.org/strain/000664.html>, 2014.
34. Aging NIO. Aged Rodent Colonies Handbook: Available Strains.
35. Rt B. Videofluoroscopic characterization of swallowing impairment in mouse models of amyotrophic lateral sclerosis and advanced aging. Columbia: Communication Science and Disorders: University of Missouri; 2014.
36. Lever TE, Gorsek A, Cox KT, O'Brien KF, Capra NF, Hough MS, Murashov AK. An animal model of oral dysphagia in amyotrophic lateral sclerosis. *Dysphagia*. 2009;24:180–95.
37. Lever TE, Simon E, Cox KT, Capra NF, O'Brien KF, Hough MS, Murashov AK. A mouse model of pharyngeal dysphagia in amyotrophic lateral sclerosis. *Dysphagia*. 2010;25:112–26.
38. Carvalho TC, Gerstner GE. Licking rate adaptations to increased mandibular weight in the adult rat. *Physiol Behav*. 2004;82: 331–7.
39. Logemann JA, Larsen K. Oropharyngeal dysphagia: pathophysiology and diagnosis for the anniversary issue of diseases of the esophagus. *Dis Esophagus*. 2012;25:299–304.
40. Logemann JA. Swallowing disorders. *Best Pract Res Clin Gastroenterol*. 2007;21:563–73.
41. Martin-Harris B, Jones B. The videofluorographic swallowing study. *Phys Med Rehabil Clin N Am*. 2008;19:769–85.
42. Lever TE, Braun SM, Brooks RT, Harris RA, Littrell LL, Neff RM, Hinkel CJ, Allen MJ, Ulsas MA. Adapting human videofluoroscopic swallow study methods to detect and characterize dysphagia in murine disease models. *J Vis Exp*, in press, 2014.
43. Berry RJ. The natural history of the house mouse. *Field Stud*. 1970;3:219–62.
44. Emond M, Faubert S, Perkins M. Social conflict reduction program for male mice. *Contemp Top Lab Anim Sci*. 2003;42:24–6.
45. Scott JP. Agonistic behavior of mice and rats: a review. *Am Zool*. 1966;6:683–701.
46. Van Loo P, Kruitwagen C, Van Zutphen L, Koolhaas J, Baumans V. Modulation of aggression in male mice: influence of cage cleaning regime and scent markers. *Anim Welf*. 2000;9:281–95.
47. Russell JA, Ciucci MR, Hammer MJ, Connor NP. Videofluorographic assessment of deglutitive behaviors in a rat model of aging and Parkinson disease. *Dysphagia*. 2013;28:95–104.
48. ADA. NDDTF: National Dysphagia Diet: Standardization for Optimal Care. Chicago: American Dietetic Association; 2002.
49. Worl J, Neuhuber WL. Enteric co-innervation of motor endplates in the esophagus: state of the art ten years after. *Histochem Cell Biol*. 2005;123:117–30.
50. Boughter JD Jr, Mulligan MK, John SJ, Tokita K, Lu L, Heck DH, Williams RW. Genetic control of a central pattern generator: rhythmic oromotor movement in mice is controlled by a major locus near Atp1a2. *PLoS One*. 2012;7:e38169.
51. Shock LA, Gallemore BC, Hinkel CJ, Szewczyk MM, Hopewell BL, Allen MJ, Thombs LA, Lever TE. Improving the utility of laryngeal adductor reflex testing: a translational tale of mice and men. *Otolaryngology*, in press.
52. Agrawal A, Rengarajan S, Adler KB, Ram A, Ghosh B, Fahim M, Dickey BF. Inhibition of mucin secretion with MARCKS-related peptide improves airway obstruction in a mouse model of asthma. *J Appl Physiol*. 1985;102(399–405):2007.
53. Agrawal A, Singh SK, Singh VP, Murphy E, Parikh I. Partitioning of nasal and pulmonary resistance changes during non-invasive plethysmography in mice (1985). *J Appl Physiol*. 2008;105:1975–9.
54. D'Ottaviano FG, Linhares Filho TA, Andrade HM, Alves PC, Rocha MS. Fiberoptic endoscopy evaluation of swallowing in patients with amyotrophic lateral sclerosis. *Braz J Otorhinolaryngol*. 2013;79:349–53.
55. Inamoto Y, Saitoh E, Okada S, Kagaya H, Shibata S, Ota K, Baba M, Fujii N, Katada K, Wattanapan P, Palmer JB. The effect of bolus viscosity on laryngeal closure in swallowing: kinematic analysis using 320-row area detector CT. *Dysphagia*. 2013;28:33–42.
56. Sugiyama N, Nishiyama E, Nishikawa Y, Sasamura T, Nakade S, Okawa K, Nagasawa T, Yuki A. A novel animal model of dysphagia following stroke. *Dysphagia*. 2014;29:61–7.
57. Ciucci MR, Russell JA, Schaser AJ, Doll EJ, Vinney LM, Connor NP. Tongue force and timing deficits in a rat model of Parkinson disease. *Behav Brain Res*. 2011;222:315–20.
58. Ciucci MR, Schaser AJ, Russell JA. Exercise-induced rescue of tongue function without striatal dopamine sparing in a rat neurotoxin model of Parkinson disease. *Behav Brain Res*. 2013;252:239–45.
59. Plowman EK, Kleim JA. Behavioral and neurophysiological correlates of striatal dopamine depletion: a rodent model of Parkinson's disease. *J Commun Disord*. 2011;44:549–56.
60. German RZ, Crompton AW, Levitch LC, Thexton AJ. The mechanism of suckling in two species of infant mammal:

- miniature pigs and long-tailed macaques. *J Exp Zool.* 1992;261:322–30.
61. Thexton AJ, Crompton AW, German RZ. Transition from sucking to drinking at weaning: a kinematic and electromyographic study in miniature pigs. *J Exp Zool.* 1998;280:327–43.
62. Ding P, Campbell-Malone R, Holman SD, Lukasik SL, Thexton AJ, German RZ. The effect of unilateral superior laryngeal nerve lesion on swallowing threshold volume. *Laryngoscope.* 2013;123:1942–7.
63. Holman SD, Campbell-Malone R, Ding P, Gierbolini-Norat EM, Griffioen AM, Inokuchi H, Lukasik SL, German RZ. Development, reliability, and validation of an infant mammalian penetration-aspiration scale. *Dysphagia.* 2013;28:178–87.

Teresa E. Lever PhD

Ryan T. Brooks MHS

Lori A. Thombs PhD

Loren L. Littrell BHS

Rebecca A. Harris BHS

Mitchell J. Allen BS

Matan D. Kadosh Under Graduate Student

Kate L. Robbins MS